Energy 238 (2022) 121663

Contents lists available at ScienceDirect

Energy

journal homepage: www.elsevier.com/locate/energy

An experimental study of a hybrid photovoltaic thermal system based on ethanol phase change self-circulation technology: Energy and exergy analysis

Yuanzhi Gao [a, *], Guohao Hu [b], Yuzhuo Zhang [c], Xiaosong Zhang [a, d, **]

[a] School of Energy and Environment, Southeast University, Nanjing, 210096, China
[b] Institute of Mechanics, Chinese Academy of Sciences, Beijing, 100190, China
[c] School of Materials Science and Engineering, Nanjing Tech University, Nanjing, 211800, China
[d] Engineering Research Center of BEEE, Ministry of Education of China, China

ARTICLE INFO

Article history:
Received 11 January 2021
Received in revised form
23 June 2021
Accepted 31 July 2021
Available online 12 August 2021

Keywords:
Photovoltaic thermal (PV/T) system
Porous media
Phase change
Energy and exergy analysis

ABSTRACT

The phase change cooling (PCC) technology combined with porous media is a promising way to enhance the performance of photovoltaic thermal (PV/T) system. Nevertheless, the application of this method is rarely mentioned in PV/T system. This paper aims to build a new phase change self-circulation (PCSC) PV/T system based on PCC technology and porous media. The system is constructed under outdoor conditions using commercial solar panel with the size of 550 mm × 460 mm × 25 mm. The performance of the system is accessed from energetic and exergetic concept under varying operating conditions (such as solar irradiance, mass flow rates, operating temperature). The obtained data shows that the proposed system is feasible with an average cooling efficiency of 34.6%, and the maximum panel temperature difference is 4.2 °C. The average daily electrical energies of the PCSC PV/T system under mass flow rates of 0.004 kg/s, 0.007 kg/s, 0.009 kg/s are 95.36 W/m^2, 94.68 W/m^2, and 95.79 W/m^2, respectively. The results are competitive compared with other works. In addition, the results also prove that the attached glass cover is beneficial to harvest thermal energy but not to electrical energy. Moreover, LCOE results indicate that the proposed system is economical compared with reference PV system.

1. Introduction

In the past few decades, energy supply system dominated by fossil fuels brings about ecosystem damage and impedes environmental sustainability [1]. Consequently, renewable and sustainable energy sources receive increasingly attention in recent years [2]. Among all the alternative energy sources, solar energy is the most suitable choice for future energy supply system with the features of easy access, unlimited reserves, and pollution-free [3,4]. Photovoltaic (PV) system can directly convert the incident solar energy into electrical energy. However, only about 20% of the incoming solar irradiation can be converted into electricity even under ideal conditions, which is still not very satisfactory [5]. If the accumulated heat cannot be dissipated in time, it will negatively impact the open circuit voltage of solar cells and threatens the long-term stable operation of the PV system [6–8]. Hence, the need for exploring and designing an efficient PV cooling system is of great importance and essential [9].

Numerous scholars have concentrated on applying advanced cooling technologies to boost the power generation efficiency of PV system. These innovative cooling techniques include but not limited to the use of phase change material (PCM), heat pipe device, nanoparticles in the coolant, thermoelectric generator, impingement jet cooling, evaporative cooling [10,11]. In particular, given that the hybrid photovoltaic thermal (PV/T) system allows dual functions (cooling PV panel and gaining thermal energy) in one unit. PV/T system is another promising cooling technology recommended by researchers.

In addition to the cooling technologies mentioned above, recently, phase change cooling (PCC) is introduced as an innovative and potential cooling strategy for combination with PV or PV/T system. The latent heat released or absorbed by PCM during phase

* Corresponding author.
** Corresponding author. School of Energy and Environment, Southeast University, Nanjing, 210096, China.
E-mail addresses: yz_shawn0213@seu.edu.cn (Y. Gao), rachpe@seu.edu.cn (X. Zhang).

https://doi.org/10.1016/j.energy.2021.121663
0360-5442/

Nomenclature

A	surface area, m^2
I	current, A
V	voltage, V
Q	coolant flow rate, L/h
T	temperature, °C
ΔT	temperature difference, °C
G	solar irradiation, W/m^2
U	voltage, V
r	energy conversion efficiency
I_{sc}	short-circuit current, A
V_{oc}	open-circuit voltage, V
P_{max}	the maximum output power, W
FF	fill factor
IP	improvement potential, W
$E\chi$	exergy rate, W
E	power, W
C_p	specific heat capacity (J/(kg°C))
m	mass flow rate (kg/s)
h	enthalpy (J/kg)
s	entropy (J/(kg. °C))

Greek symbols

η	energy efficiency
ρ	density (kg/m^3)

Subscripts

a	Ambient
oc	open circuit
sc	short circuit
in	Input
out	output
el	electrical
th	thermal
m	maximal
en	energy
s	sun
ex	exergy
gen	generation
re	reference

Abbreviation

PCSC	phase change self-circulation
PCC	phase change cooling
PV/T	photovoltaic thermal
PV	photovoltaic
EVA	ethylene-vinyl acetate copolymer
IR	infrared
SI	sustainability index
IP	improvement potential
LCOE	levelized cost of electricity
NPV	net present value

change process is hundreds of times higher than sensible heat. More importantly, PCC can achieve the decrease of the heated surface temperature variation, which is crucial for uniform cooling of solar cells [12]. Generally, PCC phase transition consists of liquid-vapor or solid-liquid cycles. From one hand, Suresh et al. [13] studied a liquid-vapor phase change cooling (evaporative cooling) technology to enhance PV panel power output. The results show that increased efficiency of 10% was achieved by cooling down the PV panel with a porous surface. Also, by incorporating a synthetic clay to the rear of the PV module, Alami et al. [14] found that the PV module temperature can be effectively reduced, and the maximum values of 19.4% and 19.1% in output voltage and power were observed. Furthermore, Nižetić et al. [15] explored the feasibility of simultaneously cooling both sides of the PV module by introducing the water spray technology (another kind of liquid-vapor phase change cooling). The experimental results indicate that the average PV panel temperature of 24 °C was obtained by cooling the front and rear sides of the PV panel at the same time. Nevertheless, in most situations, the evaporated water is transported directly to the atmosphere, which can not be recycled. This problem hindered the development of evaporative cooling, especially for those tropical climate zones. On the other hand, by attaching the solid-liquid PCM at the rear of PV panel, Maatallah et al. [16] proved that compared with conventional PV system, the PV/T-PCM system led to an improved thermal and overall efficiency of 26.87% and 40.59% respectively, along with a rise in electrical efficiency by 17.33%. Similarly, from numerical and experimental approrches, Fayaz et al. [17] comfirmed that an enhancement of 12.91% and 12.75% of electrical performance is obtained as numerically and experimentally respectively for PVT-PCM system.

From the above literature survey, it can be concluded that PCC technology is an effective method to enhance the performance of the solar PV system. In addition, PCC always undergoes an evaporation process, while various low-boiling refrigerants can be selected as coolants [12]. However, using low-boiling point coolant in liquid-vapor PCC PV/T system was not mentioned in public literature. Meanwhile, the experiment conducted by Ahmed et al. [18] pointed out that using porous media in PV/T system leads to a positive impact. Nevertheless, to the authors' knowledge, the attempts of simultaneously using porous material and low-boiling coolant in PCC PV/T system to realize working medium circulation and obtain thermal energy also have been rarely reported. Furthermore, in our previous study, an active PCC system was established for flat PV cooling [19], but the possibility of building a PV/T system to enhance overall energy efficiency was neglected. Accordingly, the current research tackles the challenge of building a phase change self-circulation (PCSC) PV/T system using PCC technology. The findings of the present work also provide novel insights into the newly designed PCSC PV/T system using low boiling point liquid (ethanol) as working medium and realize the self-circulation of working fluid with the aid of porous media. The effect of the glass cover, solar irradiation, water flow rates on the fluence of the system is detailed discussed. Besides, economic analysis is conducted to analyze the economic performance of the system.

2. Experimental setups and methods

The essential equipment used in this system mainly comprises two PV modules (one considered as a reference PV module, the other fabricated as PCSC PV/T module), a water circulation system, data testing and acquisition system. The specific technical parameters of the PV module are listed in Table 1. Furthermore, to compare the performance of glazed and unglazed PCSC PV/T system, a glass cover is attached at the front of PV/T module.

2.1. The PCSC PV/T module

As previously described, this paper aims to establish a self-circulation phase change PV/T system. In order to evaluate the performance of the proposed system, two prototypes of the PCSC

Table 1
Technical parameters of mono-crystalline silicon PV module (AM1.5, 1000 W/m^2 and 25 °C).

Technical parameters	Unit	Value
Model	–	SUN-30
Maximum power output	W	30
Maximum power voltage	V	17.5
Maximum power current	A	1.71
Open circuit voltage	V	21.5
Short circuit current	A	1.94
Fill factor	–	73%

PV/T module are designed and fabricated, namely the unglazed and glazed PCSC PV/T module. In addition, an original PV module is also prepared to make a comparison with the PV/T system. The detailed structural design and cross section view of the considered system are illustrated in Fig. 1 and Fig. 2. In the following elaboration, the three different Cases 1, 2, 3 are referring to reference PV module, unglazed PCSC PV/T module, and glazed PCSC PV/T module.

Case 1. A conventional PV panel (SUN-30, Beijing Tianzhu Yangguang Solar Energy Technology Co., China) with a maximum power output of 30 W is used as a reference case. The PV module has 12 pieces of solar cells that are connected in series and parallel. The detailed composition structure is shown in Fig. 1 (a).

Case 2. The schematic of the unglazed PCSC PV/T module is presented in Fig. 1 (b). The core part of the PV/T module is a combination of a classical PV module, and the modified part. The modified part consists of the porous medium, copper collector tube and V-shaped sump. The non-woven fiber fabric is selected as the porous medium and attached at the rear plate of the PV panel using silica gel with high thermal conductivity. Several V-shaped sumps made up of copper foil are also bonded to the backside of PV module, which acted as a liquid reservoir. In the meantime, 5 copper pipes are fixed at the aluminum frame of the PV panel by drilling holes to collect the latent heat released by ethanol vapor during the phase change process. A tempered glass plate (mm) is chosen for encapsulating the PV panel to form a closed system. To ensure no leakage issues, the gap between the glass cover and the aluminum frame is filled with silicone sealant. Once the closed system was prepared, the ethanol liquid is injected into the V-shaped sump through the pre-defined injection holes.

The complete phase change self-cycling process consists of two parts: the first part is the liquid to vapor phase transition. The ethanol liquid in the V-shaped sump is absorbed into the porous material by capillary force. When sunlight hits the surface of the PV panel, the uprising temperature makes the ethanol liquid evaporate and resulting in a lower PV temperature. The second part is the vapor to liquid phase transition. The evaporated ethanol vapor condenses on the cold surface of the copper collector tube and transfers the latent heat to the water inside the collector tube. Under the action of gravity, the droplets finally drop into the V-shaped sump and reabsorbed by the porous medium. In this way, the purpose of self-circulation is achieved. During the evaporation process of ethanol, the porous materials can effectively enhance the heat and mass transfer, which is confirmed in a previous study [20].

Case 3. As shown in Fig. 1 (c), to investigate the influence of glass cover on the PCSC PV/T system, clear borosilicate glass with high transmission efficiency for solar irradiation is placed over the PV panel. Several U-shaped clips are used for joining the glass cover together with the PV panel. The thickness of the air gap between the PV surface and glass cover is 30 mm.

2.2. Experimental setup

Except for the PCSC PV/T module and reference PV module, other support systems include water circulation and data measurement system. The schematic and photographic view of the tested facility is presented in Fig. 3. The tests are performed on the days with clear and stable conditions from 10:00 a.m. to 2:45 p.m.

As Fig. 3 (a) displays, the water circulation system comprises of a water pump, water storage tank, heat exchange water tank, flow meter, and the connecting pipelines. The detailed parameters of the system are summarized in Table 2. To improve the condensation effect, a spiral heat exchanger is immersed in the heat exchanger tank to maintain the water temperature at a low level.

To investigate the impact of flow rates on the PCSC PV/T performance, different mass flow rates of 0.004 kg/s, 0.007 kg/s, 0.009 kg/s are considered. The flow rates of cooling water can be regulated by the valve. To reduce the heat loss of the system, all external circulation pipes and water tanks are covered with insulation materials.

2.3. The data measurement and acquisition system

The operating parameters of the system monitored by the corresponding measuring equipment are shown in Table 3. To measure the temperature variation of the system, K-type thermo sensors are used to test the temperature data, and the data logging interval was 1s. Specifically, the measuring points' locations of the PV panel is depicted in Fig. 4. The current, voltage, and power output of the PV modules are collected by an I–V curve instrument with a scanning interval of 15 min.

An infrared (IR) thermal camera is prepared to photography the IR color images of the PV units. A global pyranometer is fixed on the supporting frame with the same inclination angle as the PV panels to measure the solar radiation intensity. Then, the millivolt signal output from the pyranometer is recorded by the ART data collector.

2.4. Experimental procedure

The specific operation steps during the experiment are as follows:

a Turn on the power supply switch of the system and confirm whether each test instrument is in normal working condition.
b Turn on the data acquisition system, observe whether the data acquisition system is normal, and set the data sampling interval.
c Adjust the flow rates to the required values and let water flow for a period to ensure the stability of the water flow during the experiment.
d Before the experiment time, remove the mirror aluminum plate (as a light shield) over the PV panel and wipe the dust from the surface of the PV panel.
e Start the experiment, use the PC to record and save the experimental data, and use the IR camera to collect the images of the system.
f. After the experiment, save and copy the experimental data, turn off the power supply, and restore the system to the initial state.

2.5. Analysis methodology

2.5.1. Energy analysis

From the perspective of energy, the control volume of the PCSC PV/T module is considered as the joining of the thermal collector and PV module. According to the first law of thermodynamics, the

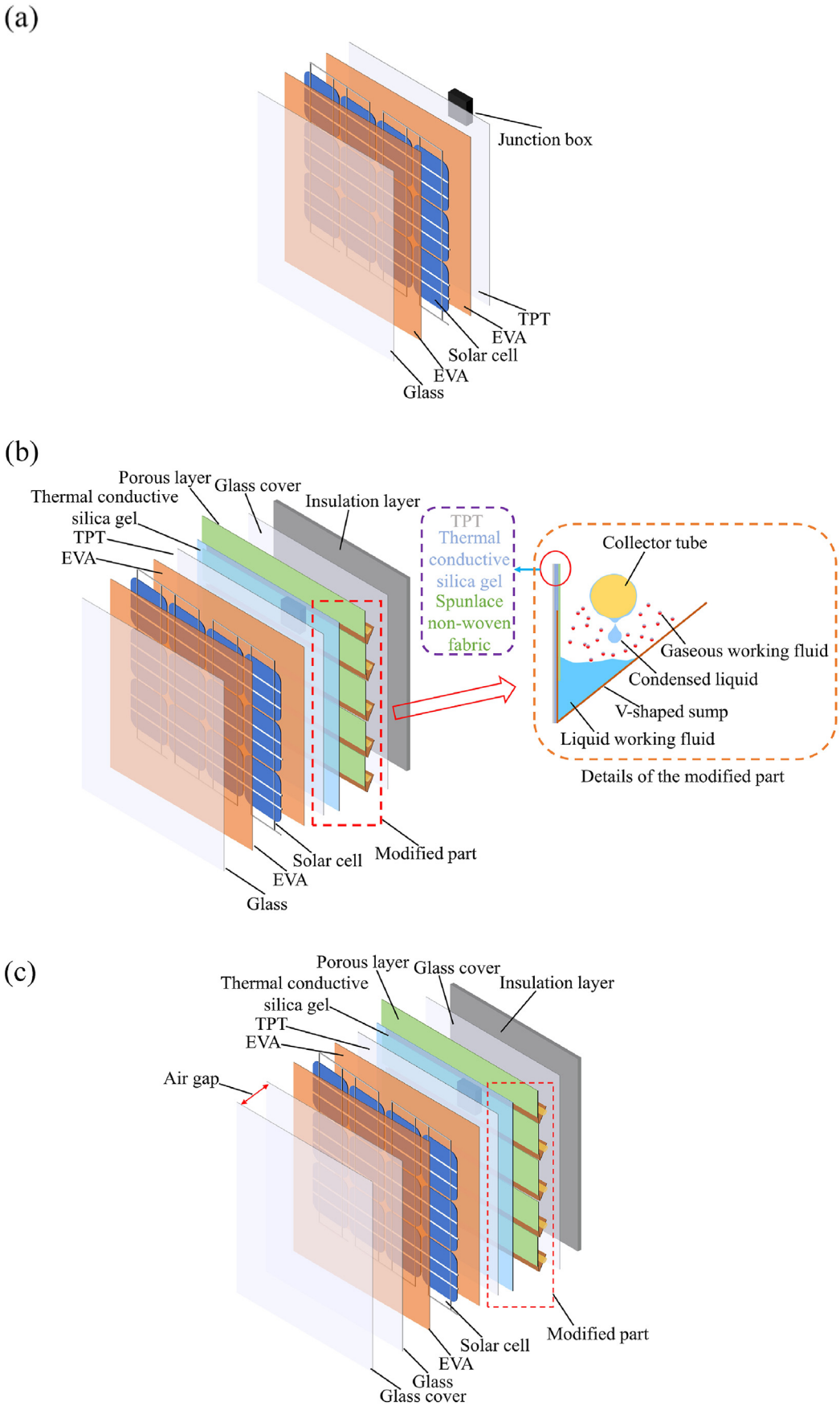

Fig. 1. Schematic of the tested systems (a) PV module only, (b) unglazed PCSC PV/T module, (c) glazed PCSC PV/T module.

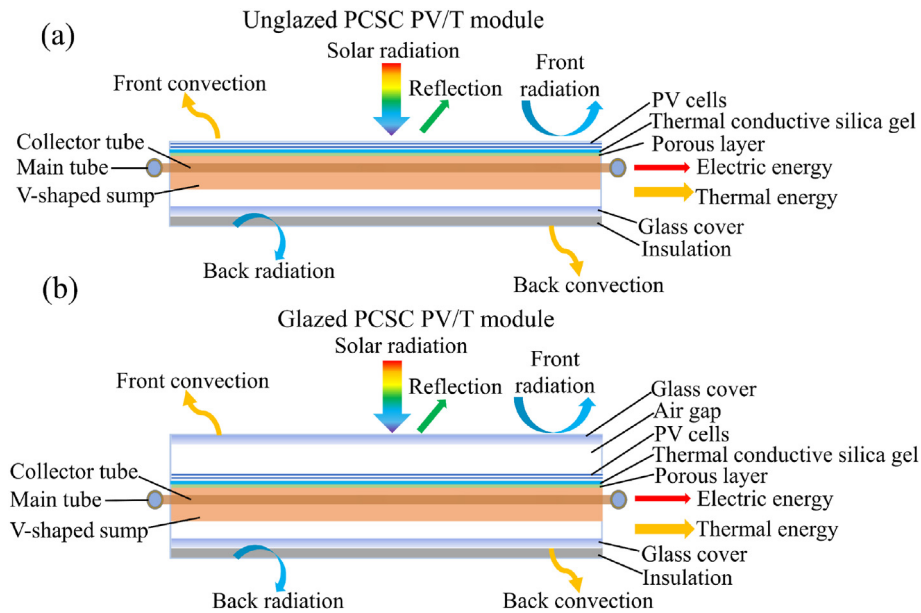

Fig. 2. Cross section views of (a) unglazed PCSC PV/T module (b) glazed PCSC PV/T module.

overall energy expression of the proposed PCSC PV/T system can be written as:

$$\sum E_{in} = \sum E_{out} \tag{1}$$

Fig. 5 (a) shows that the energy flowing into the control volume of the system comprises two different parts: the energy inputted from the sun and the heat transfer fluid. Thereby, the total input energy rate can be defined as:

$$\sum E_{in} = E_{sun,\ in} + E_{fluid,\ in} \tag{2}$$

where $E_{sun,\ in}$ and $E_{fluid,\ in}$ stand for the input energy of the sun and the heat transfer fluid, respectively. The expression of input solar energy is given by:

$$E_{sun,\ in} = G \cdot A \tag{3}$$

where G and A refer to the solar illumination intensity and the surface area of the PV module.

Similarly, the output energy of the control volume can be expressed as:

$$\sum E_{out} = E_{el,\ out} + E_{fluid,\ out} \tag{4}$$

where, $E_{el,\ out}$ and $E_{fluid,\ out}$ indicate the output energy of electric and the heat transfer fluid.

$E_{el,\ out}$ is the output power produced by the PV unit, which can be decided as [21]:

$$E_{el,\ out} = V_{oc} \cdot I_{sc} \cdot FF \tag{5}$$

where, V_{oc}, I_{sc} and FF refer to the open circuit voltage, short circuit current and fill factor (FF) of the PV unit, respectively. $V_{oc}$and I_{sc} are provided by the supplier. FF is defined as the ratio of the product of current and voltage to the product of short circuit current and open circuit voltage when the solar cell has the maximum output power [22], FF can be calculated as:

$$FF = \frac{V_m \cdot I_m}{V_{oc} \cdot I_{sc}} \tag{6}$$

In this equation, V_m, I_m are the voltage and current at the maximum power point, respectively.

In addition, the useful thermal energy (E_{th}) produced by the PCSC PV/T collector is considered as a fixed relationship up to the features of the working fluid:

$$E_{th} = E_{fluid,\ out} - E_{fluid,\ in} = m_{fluid} \cdot C_{p,\ fluid} \cdot \left(T_{fluid,out} - T_{fluid,in}\right) \tag{7}$$

where, $m_{fluid}, C_{p,\ fluid}$, $T_{fluid,out}$ and $T_{fluid,in}$ are the useful heat absorbed by the PV/T collector, the mass flow rate of heat transfer fluid, outlet and inlet temperature of heat transfer fluid, respectively.

Thus, the electrical and thermal efficiency of the PV/T system are written as [23]:

$$\eta_{el} = \frac{E_{el,\ out}}{E_{sun,\ in}} = \frac{P_{max}}{G \cdot A} = \frac{V_{oc} \cdot I_{sc} \cdot FF}{G \cdot A} \tag{8}$$

$$\eta_{th} = \frac{E_{th}}{E_{sun,\ in}} = \frac{m_{fluid} \cdot C_{p,\ fluid} \cdot \left(T_{fluid,out} - T_{fluid,in}\right)}{G \cdot A} \tag{9}$$

Then, the overall efficiency can be expressed by η_{el} and η_{th} as in Eq. (10):

$$\eta_{en} = \eta_{th} + \frac{\eta_{el}}{r} \tag{10}$$

Since the grade of electric energy is higher than that of thermal energy. The parameter of r is used to describe the conversion efficiency, which considers the electric energy into equivalent thermal energy. The specific conversion value is 0.38 [23].

2.5.2. Exergy analysis

As shown in Fig. 5 (b), from the second law of thermodynamics, the exergy efficiency is used to describe the 'quality' of the energy

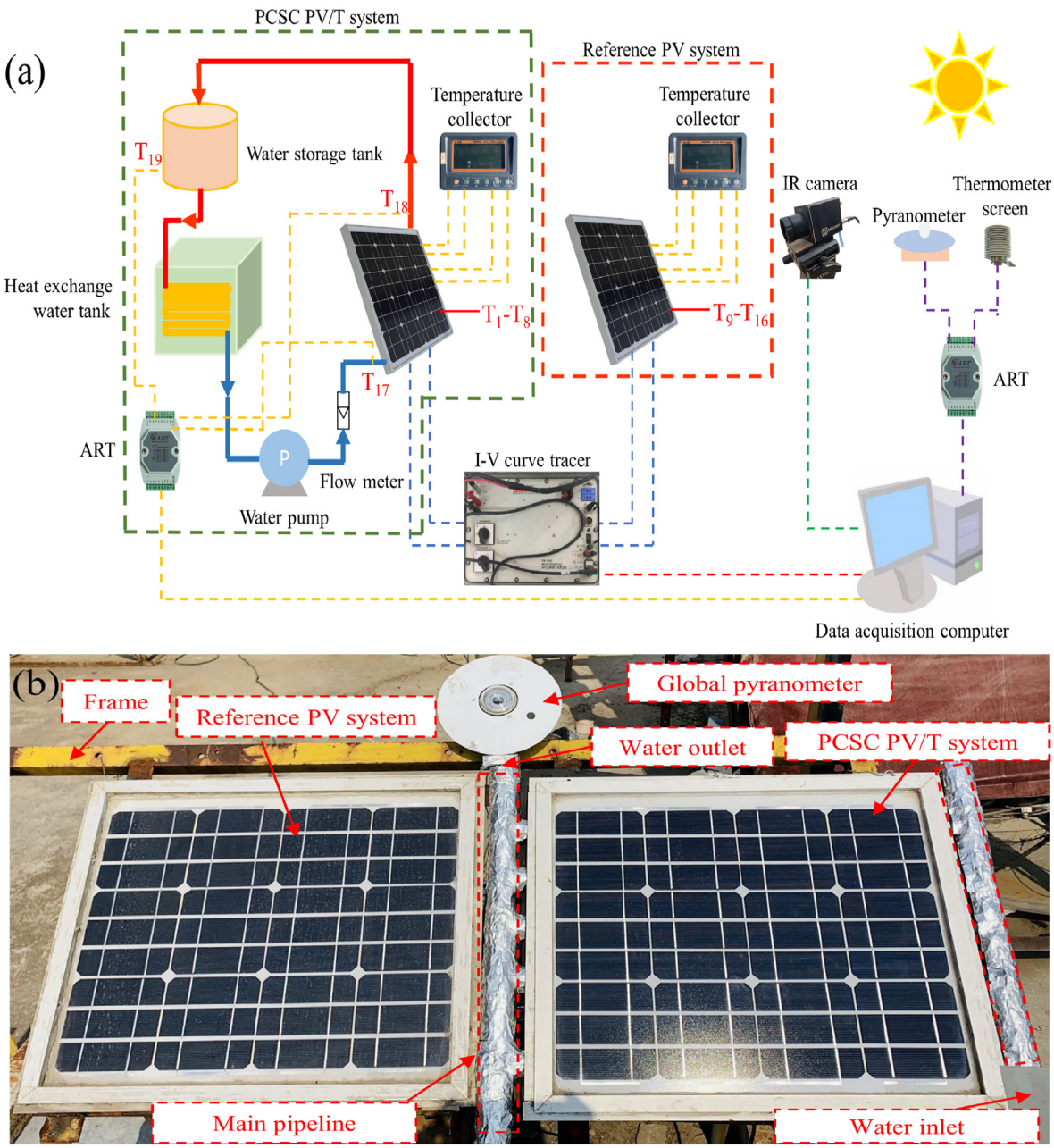

Fig. 3. The pictures of (a) the schematic of the facility and (b) a real picture of the experimental setup.

Table 2
Parameters of the PCSC PV/T system.

Parameter	Unit	Value	Error	Materials
Water pump	W	46	–	–
Heat exchange water tank	L	48	–	Stainless steel
Water storage tank	L mm	12	–	Polyethylene
Circulating water pipeline	mm	Ø12 * 1	±0.1	Polyethylene
Heat exchange tube	mm	Ø12 * 1	±0.1	Copper
Glass cover (thickness)	mm	4	–	Borosilicate glass
Insulation material (thickness)		15	–	Rubber insulation cotton

conversion efficiency. Similar to that of energy expression, the overall exergy balance equation is expressed as:

$$\sum E\chi_{in} - \sum E\chi_{out} = \sum E\chi_{loss} \tag{11}$$

Table 3
Measuring equipment and their accuracies.

Measuring equipment	model	accuracy	Monitoring target/purposes
K-type thermocouples	5 TC-TT-K-36-36	±0.1 °C	Measure the temperature data of the system
Four-channel temperature collector	AZ88598	±0.1 °C	Collect and save the temperature data
I–V curve instrument	DS-100c	current accuracy ±0.5%, voltage accuracy ±0.5%,	Measure the current, voltage, and power of the PV panel
Thermal infrared (IR) camera	MAG62	±2 °C	Evaluate the temperature distribution of the PV panel
Global pyranometer	PSP	<10 W/m^2	Measure the incident solar irradiation
ART data collector	DAM3038	±0.2%	Record the temperature of inlet, outlet, water storage tank and solar irradiation data
Flow meter	LZB-10	accuracy ± 4%	Measure the flow rates of water

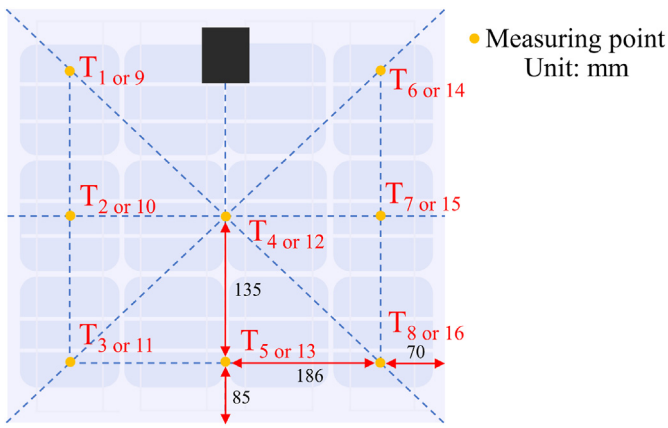

Fig. 4. The positions of the measuring points (1–8 for reference PV module and 9–16 for PCSC PV/T module).

$$E\chi_{sun,in} + E\chi_{fluid,in} = E\chi_{el,out} + E\chi_{fluid,out} + \sum E\chi_{loss} \tag{12}$$

Moreover, the input exergy of the sun is decided as [24]:

$$\sum E\chi_{in} = E_{sun,\ in} = G \cdot A\left[1 - \frac{4}{3}\left(\frac{T_a}{T_s}\right) + \frac{1}{3}\left(\frac{T_a}{T_s}\right)^4\right] \tag{13}$$

where T_a and T_s refer to the ambient and sun temperature, respectively. The difference exergy of the heat transfer fluid can be defined as:

$$E\chi_{fluid,out} - E\chi_{fluid,in} = m_{fluid}\Big[\times \left(h_{fluid,out} - h_{fluid,in}\right) - T_a\left(s_{fluid,out} - s_{fluid,in}\right)\Big] \tag{14}$$

In which, h_{fluid} and s_{fluid} are enthalpy and entropy of the heat transfer fluid, respectively. The changes of entropy and enthalpy of the PCSC PV/T system can be arranged as [25]:

$$\Delta h = h_{fluid,out} - h_{fluid,in} = C_{p,\ fluid}\left(T_{fluid,out} - T_{fluid,in}\right) \tag{15}$$

$$\Delta s = s_{fluid,out} - s_{fluid,in} = C_{p,\ fluid}\ \ln\left(\frac{T_{fluid,out}}{T_{fluid,in}}\right) \tag{16}$$

Therefore, the exergy of electrical and thermal can be calculated using the following equations:

$$E\chi_{el,out} = E_{el,out} \tag{17}$$

$$E\chi_{th} = m_{fluid} \cdot C_{p,\ fluid}\left[\left(T_{fluid,out} - T_{fluid,in}\right) - T_a\ \ln\left(\frac{T_{fluid,out}}{T_{fluid,in}}\right)\right. \tag{18}$$

Hence, combining Eq. (13), Eq. (17), and Eq. (18) yields the exergy loss of the system:

$$\sum E\chi_{loss} = E\chi_{sun,in} - E\chi_{th} - E\chi_{el,out} \tag{19}$$

Finally, the electrical, thermal, and overall exergy efficiencies of the PCSC PV/T system can be calculated using the following three equations [26]:

$$\eta_{ex,el} = \frac{E\chi_{el,\ out}}{E\chi_{sun,\ in}} = \frac{V_{oc} \cdot I_{sc} \cdot FF}{G \cdot A\left[1 - \frac{4}{3}\left(\frac{T_a}{T_s}\right) + \frac{1}{3}\left(\frac{T_a}{T_s}\right)^4\right]} \tag{20}$$

$$\eta_{ex,th} = \frac{E\chi_{th}}{E\chi_{sun,in}} = \frac{m_{fluid} \cdot C_{p,fluid}\left[\left(T_{fluid,out} - T_{fluid,in}\right) - T_a \ln\left(\frac{T_{fluid,out}}{T_{fluid,in}}\right)\right.}{G \cdot A\left[1 - \frac{4}{3}\left(\frac{T_a}{T_s}\right) + \frac{1}{3}\left(\frac{T_a}{T_s}\right)^4\right]} \tag{21}$$

$$\eta_{ex} = \frac{\frac{E\chi_{el,\ out}}{r} + E\chi_{th}}{E\chi_{sun,\ in} + P_{pump}} \tag{22}$$

In this equation, P_{pump} is the power consumed by the water pump. In this system, the parasitic energy consumption of the water pump is the external exergy input.

The entropy generation of the PCSC PV/T system denoted as [27]:

$$S_{gen} = \frac{\sum E\chi_{loss}}{T_a} \tag{23}$$

The exergetic concept of sustainability index (SI) [27] and improvement potential (IP) [19], which used to describe the maximum improvement for the PCSC PV/T system, could be determined as:

$$SI = \frac{1}{1 - \eta_{ex}} \tag{24}$$

$$IP = (1 - \eta_{ex}) \cdot \sum E\chi_{loss} \tag{25}$$

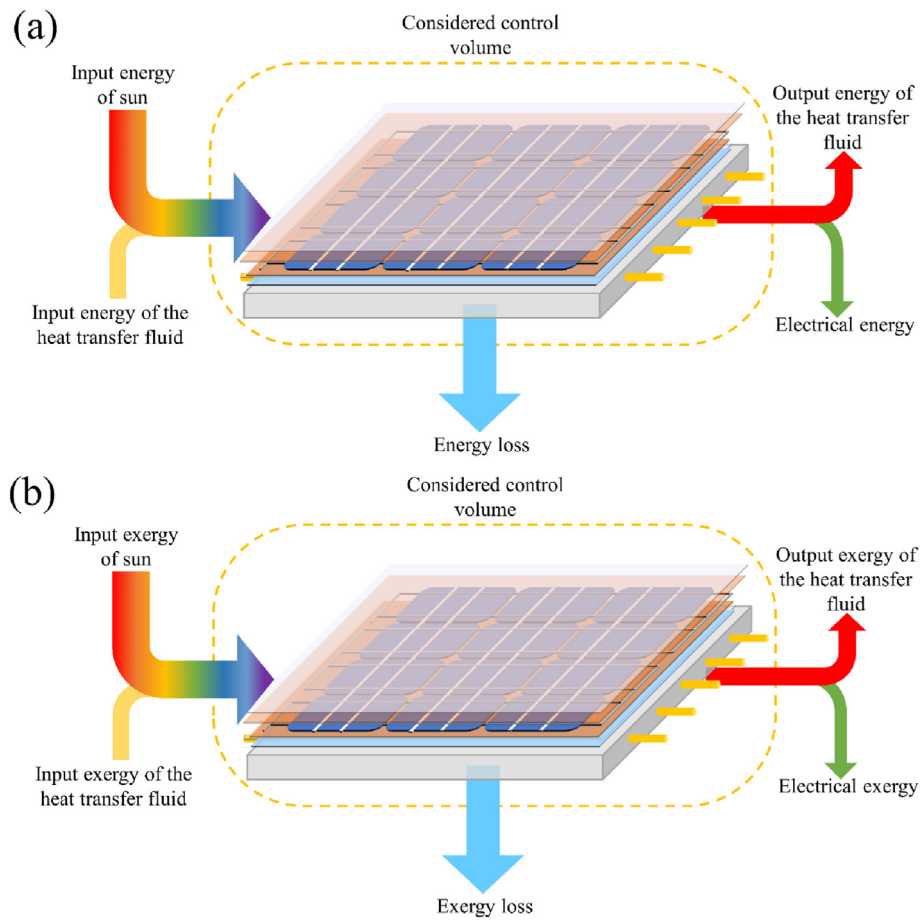

Fig. 5. The diagram of (a) energy flow and (b) exergy flow.

2.5.3. Uncertainty analysis

To guarantee the accuracy of the experimental results, uncertainty analysis is conducted. The uncertainty of the experiment can be determined using the following equation [28]:

$$U_Z = \sqrt{\left(\sum_{i=1}^{n}\left[\frac{\partial Z}{\partial x_i}U_i\right]^2\right)} \tag{26}$$

where x_i and U_i represent the direct testing parameters (such as mass flow rates, temperature, solar irradiation, etc.) and the associated uncertainty of measuring instruments are listed in Table 3.

Based on this analysis, the calculated uncertainties of the thermal, electrical and overall efficiency are 4.47%, 2.12% and 4.94%, respectively. The obtained maximum uncertainties for all parameters are less than 5% which indicates the reliability of the experimental data.

3. Results and discussion

3.1. Weather conditions

To avoid undesirable meteorological conditions, the experiments are performed on sunny days. Fig. 6 displays the variations of solar irradiance and ambient temperature during a typical experimental day. It is noted that the variation range of solar radiation intensity is approximately 500 W/m^2 to 950 W/m^2, with an average value of 825 W/m^2. The ambient temperature increases from about 14 °C in the morning to 21 °C at the end of the test. The daily fluctuation of the weather data during the whole experimental period is relatively small and stable.

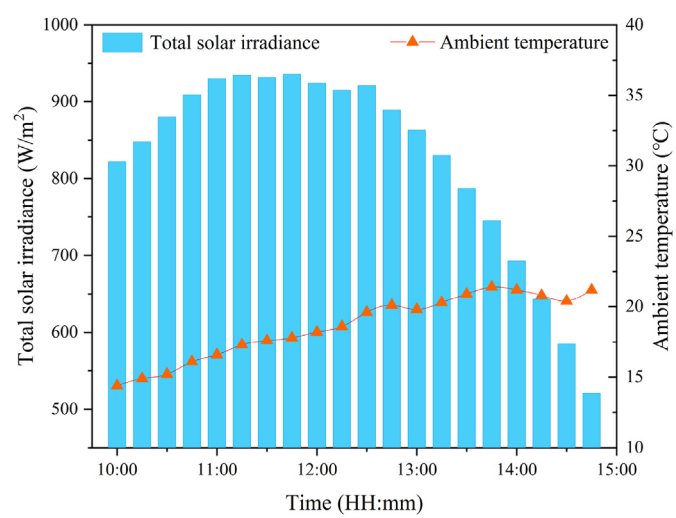

Fig. 6. The weather conditions during the experimental time.

3.2. Temperature profiles analysis of system

The temperature change curves for each measurement point are

illustrated in Fig. 7 (a) and Fig. 7 (b). According to Fig. 7 (a) and Fig. 7 (b), the temperature of both PV panels shows a similar trend in the initial stage. During the second 15-min interval, the temperature of the reference PV module and PCSC PV/T module rises up quickly to around 45 °C and 30 °C, respectively. This phenomenon can be explained as, under the protection of the light shield, the temperature of the PV panels is maintained at a lower level before the experiment start. Once the light shield is removed, the PV panel temperature dramatically increases under the influence of solar irradiation. After this stage, the PV panel temperature shows a dynamic change as the experiment goes on.

Simultaneously, the maximum temperature difference (among the 8 test points) of the PCSC PV/T module is 4.2 °C, which is obviously smaller than the reference PV module of 5.7 °C. Moreover, the reference PV system's temperature fluctuation is larger than that of the previous system, which indicates that the PCSC PV/T system has a strong anti-interference ability to resist environmental fluctuations, and even temperature distribution can be obtained by using this technique. During this period, the outlet temperature of water raises from 12.3 °C to 22.3 °C.

Fig. 7 (c) presents the cooling temperature difference between the reference PV module and PCSC PV/T module, and also the cooling efficiency of the PCSC PV/T module. The maximum temperature difference and the average temperature drop difference of the PCSC PV/T module relative to the reference PV module is 21.6 °C and 17.6 °C, respectively. Meanwhile, the maximum and the average cooling efficiency of the system are 37.8% and 34.6%, respectively.

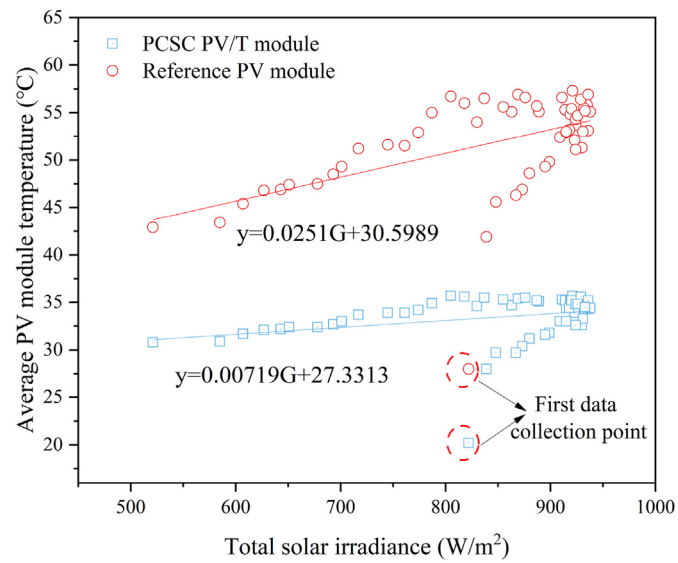

Fig. 8. The average temperature of the PV module as a function of total solar irradiance.

From Fig. 8, it can be clearly revealed that for both PV modules, the average PV panel's temperature shows a linear relationship with the incident solar radiation intensity. To be more specific, the

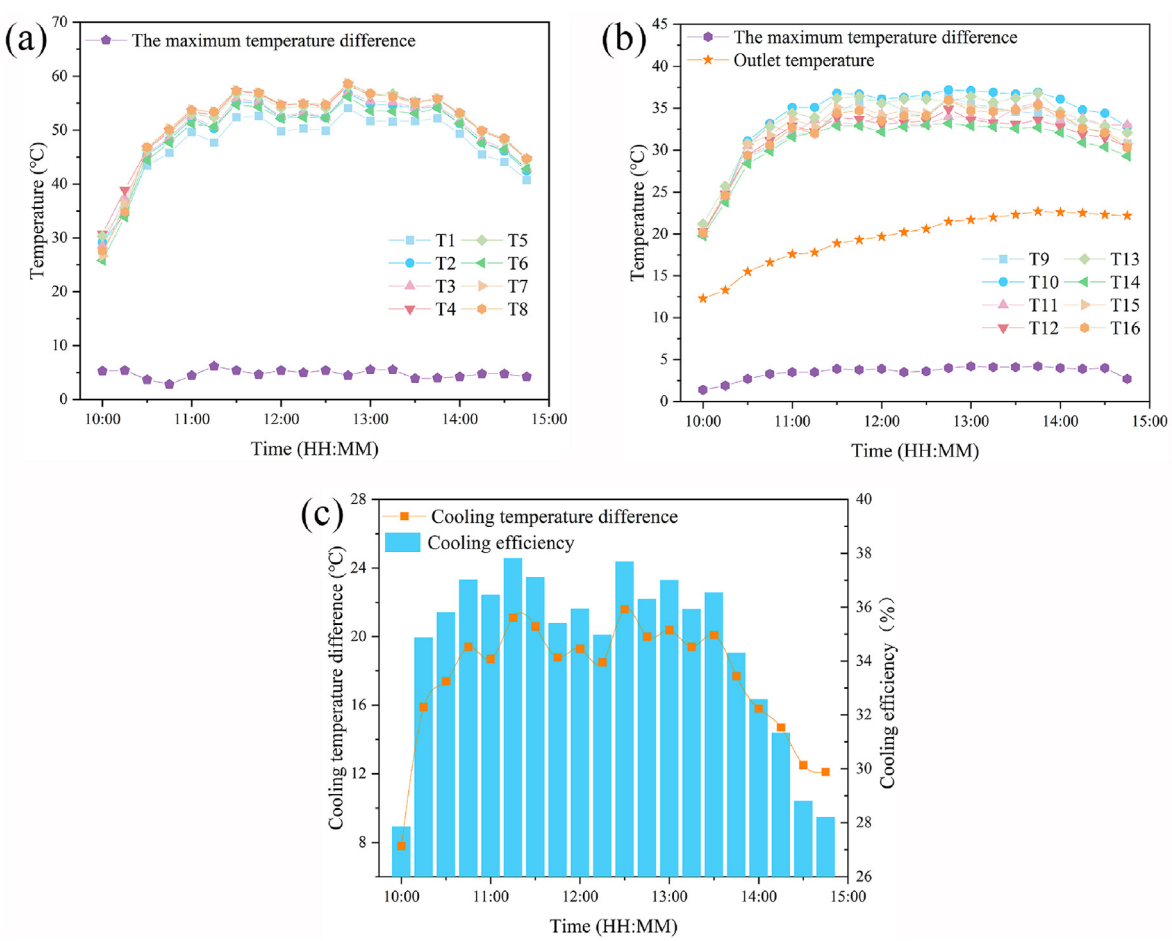

Fig. 7. Temperature changes of (a) reference PV module (b) PCSC PV/T module (c) and cooling efficiency and cooling temperature difference.

corresponding coupling relationships of the reference PV module and PCSC PV/T module are described by the following equations:

$$T_{re,PV} = 0.0251G + 30.5989 \tag{27}$$

$$T_{PCSC,PV/T} = 0.00719G + 27.3313 \tag{28}$$

From the above formulas, it is evident that, for every 100 W/m^2 increments, the increased temperatures for reference PV module and PCSC PV/T module are 2.5 °C and 0.7 °C, respectively. As illustrated in Fig. 8, particular attention should be given to the first data collection point. The occurred of the two points is that the data is recorded when the light shield is just removed.

3.3. The energy analysis of the system

The yielded electric power of the two considered systems is shown in Fig. 9 (a). It is observed that during the whole time of the experiment, the electricity produced by the PCSC PV/T module is much higher than that of the reference PV module. The maximum and minimum power differences of the two systems are 2.5 W and 1.1 W, respectively, with an average value of 2 W. This confirms that the application of PCSC technology could effectively reduce the output power drop.

Fig. 9 (b) depicts the variation of short circuit current and open circuit voltage of the two systems. It is noticed that the short circuit current difference between the reference PV module and the PCSC PV/T module does not change much, whereas the open circuit voltage of the PCSC PV/T module is higher than that of the reference PV module. This implies that the open circuit voltage of the solar cells is more sensitive to the increased temperature. Fig. 9 (c) reflects the electric power produced by the reference PV module and PCSC PV/T module as a function of the solar irradiance. The results show that the power output of the PCSC PV/T module is superior to that of the reference case. An approximately linear relationship between PV panel power output and solar irradiation intensity can be obtained by fitting the data points:

$$P_{re,PV} = 0.0202G + 3.7143 \tag{29}$$

$$P_{PCSC,PV/T} = 0.0232G + 3.2352 \tag{30}$$

From the above two equations, it is evident that the power generated by both PV modules tends to increase with the intensity of solar irradiation. The competitiveness of the PCSC PV/T system is much higher than the uncooled PV module.

The variations of electrical energy conversion efficiency of the two systems under different mass flow rates are plotted in Fig. 10. The electrical efficiencies of the reference PV module and PCSC PV/T module present a similar variation trend, which decreases at first, then reaches the lowest point near noon, and finally increases. Obviously, the electrical efficiency of the PCSC PV/T module is higher than the reference PV module's efficiency in all considered cases. This can be attributed that the intensity of the solar radiation increases with the experimental time and leads to a progressive decline in the conversion efficiency of the solar cells. The relative

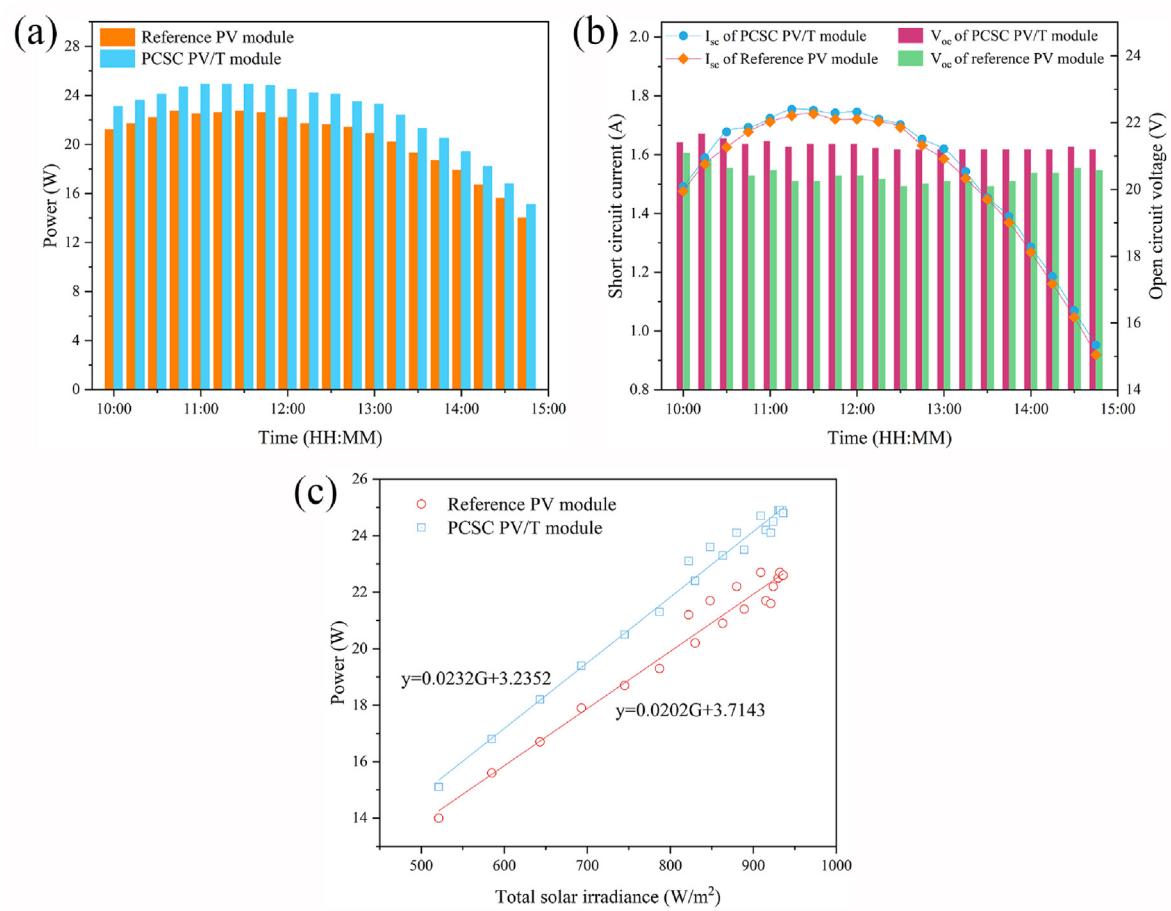

Fig. 9. The variation of the tested systems of (a) power output (b) short circuit current and open circuit voltage (c) relationship between total solar irradiance and power output.

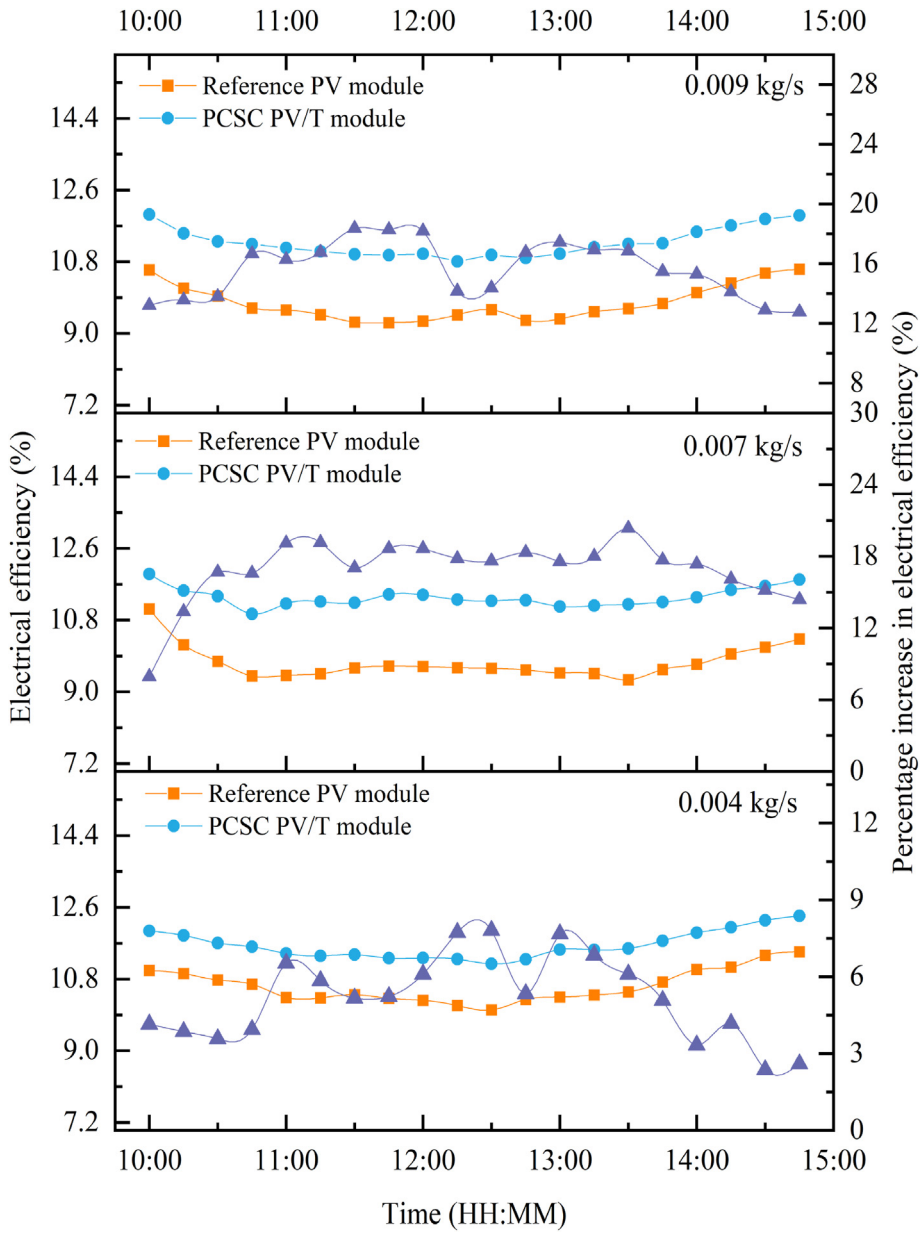

Fig. 10. The electrical efficiency of the tested systems under different mass flow rates.

increase of the electrical efficiency is also illustrated in Fig. 10. Compared with the reference PV module, the average percentage increase in electrical efficiency under the three considered mass flow rates of 0.004 kg/s, 0.007 kg/s, 0.009 kg/s are 9.74%, 16.87%,15.06%, respectively.

Considering the mass flow rates of 0.004 kg/s as an example, by varying the total solar irradiance, the corresponding relationships of the reference PV module and PCSC PV/T module can be obtained, as reported in Fig. 11. Moreover, the following equations are used to describe the relationships:

$$E_{\mathrm{re,PV}} = -0.0037G + 13.4651 \tag{31}$$

$$E_{\mathrm{PCSC,PV/T}} = -0.0030G + 13.9735 \tag{32}$$

It can be noted that, for both systems, the solar irradiation intensity shows a certain negative linear relationship with electrical efficiency. In contrast, the trend of the electrical efficiency of the PCSC PV/T system with the radiation intensity is more moderate than that of the reference PV system.

In this study, the percentage decrease in electrical efficiency per 1 °C increase in solar cell temperature is determined by calculating the PV modules' electrical efficiency and average temperature at the start or peak period. Table 4 summarizes the gained results in different studies. From the table, it is worth to notice that for every 1 °C increase in temperature, the percentage decrease in this work is 0.05%, which is consistent with the results of other scholars [29–31].

The overall energy variation trends of the proposed system with the experimental time are demonstrated in Fig. 12 (a). As shown in the figure, the system reaches its highest overall energy efficiency of 68.3% under the flow rate of 0.004 kg/s, and the considered system reaches its maximum thermal efficiency of 36.9% at the same time. Hence, it is also interesting to find out that the variation

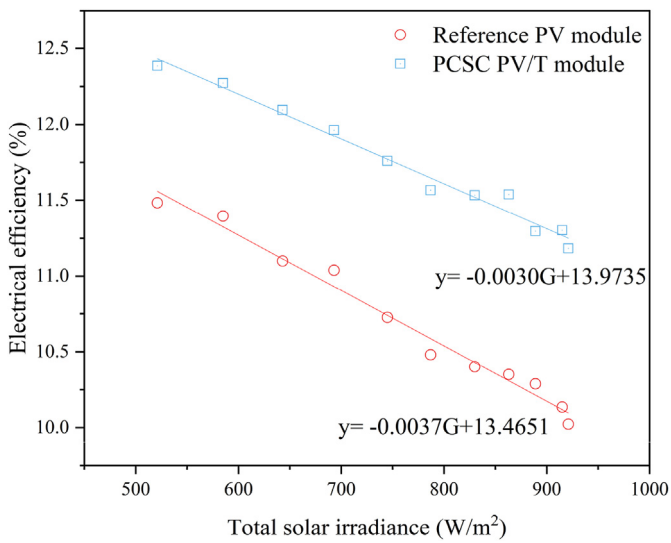

Fig. 11. The electrical efficiency as a function of the total solar irradiance.

of overall energy efficiency is consistent with thermal efficiency variation, which contributes the most part of the obtained energy. Fig. 12 (b) illustrates the gained energy of the PCSC PV/T system and reference system under different flow rates. According to the figure, it is clear to see that the electrical energy produced by the PCSC PV/T system is significantly higher than the reference PV module, which is seriously influenced by the operating temperature. Besides, the overall energy of the PCSC PV/T module increases, with the increases of mass flow rates of cooling water.

To compare the average electrical power with other works. Fig. 13 shows the obtained values in PCSC PV/T system (this study), PV/T PCM system (Kazemian et al. [32]), and PV/T PCM system (Kazemian et al. [33]). This result show that using PCC technology can effectively improve the electrical power of the proposed PV/T system.

3.4. The exergy analysis of the system

The main purpose of this section is to perform an exergetic analysis from the point of the second law of thermodynamics. Fig. 14 presents the variations of daily input exergy, exergy loss of the PCSC PV/T module, and the reference PV module. As can be seen from the figure, the input sun exergy increases first, then reaches its maximum value of 218.14 W, and finally drops its minimum value of 121.33 W. The exergy losses of the reference PV module and PCSC PV/T module show a similar variation trend compared to that of the input sun exergy. The exergy loss of the reference PV module is significantly higher than that of the PCSC PV/T module, which proves that the proposed PCSC PV/T module is more effective than the reference PV module.

Fig. 15 highlights the changes in exergy power of the PCSC PV/T system compared with the reference PV system. The data indicated that, for the PCSC PV/T module, the exergy power of the thermal is much lower than the exergy power of electrical. In terms of the extent to which energy is efficiently converted, this result confirmed that the majority of the electrical exergy could be converted into useful exergy, compared with the thermal exergy [34]. Meanwhile, the average exergies of thermal and electrical for PCSC PV/T system are 5.30 and 95.36 W/m^2, respectively. Furthermore, compared with the PCSC PV/T module, the corresponding value of electrical exergy of the reference PV module is 87.26 W/m^2.

The changes in SI and entropy generation for the PCSC PV/T and PV systems are plotted in Fig. 16 (a). It is easy to conclude that the SI of the PCSC PV/T module is considerably higher than the reference PV module, which means that the PCSC PV/T system is more feasible than the reference PV system. The average SI indexes of the reference PV module and PCSC PV/T module are 1.11 and 1.43, respectively. In contrast, the entropy generation of the PCSC PV/T module is lower than the reference PV module. The reason can be explained as: the input exergy can be effectively used by the PCSC PV/T module, and the generated entropy is smaller than that of the reference PV module. Fig. 16 (b) shows the changes of IP of the two systems. It is found that the variation of the IP shows a good linear relationship with the variation of solar radiation. Moreover, it is

Table 4
Efficiency reduction rate of PV modules in different studies for every 1 °C rise in temperature.

Ref.	Operating temperature (°C)		Electrical efficiency (%)		Percentage decrease in electrical efficiency per 1 °C increase in cell temperature
	Start	Peak period	Start	Peak period	
[29]	37	65	10.3	9	0.05
[30]	25	44	15.7	15.2	0.03
[31]	32.1	88.1	7.63	4.5	0.06
Present work	20.2	35.7	12.01	11.18	0.05

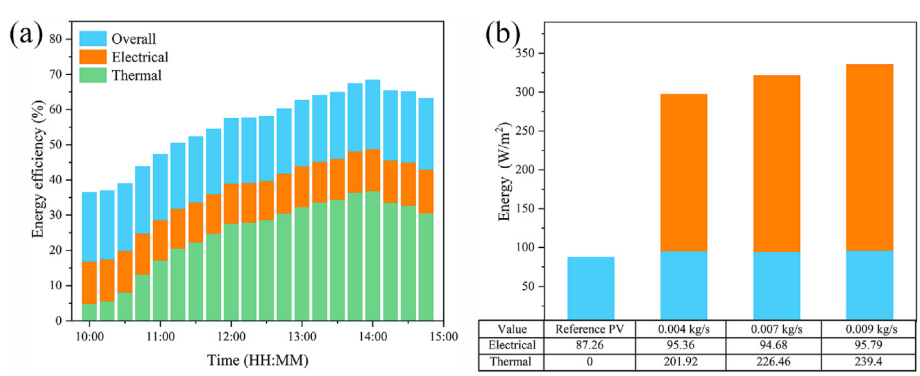

Fig. 12. The variations of PCSC PV/T system (a) energy efficiency (b) total energy gained.

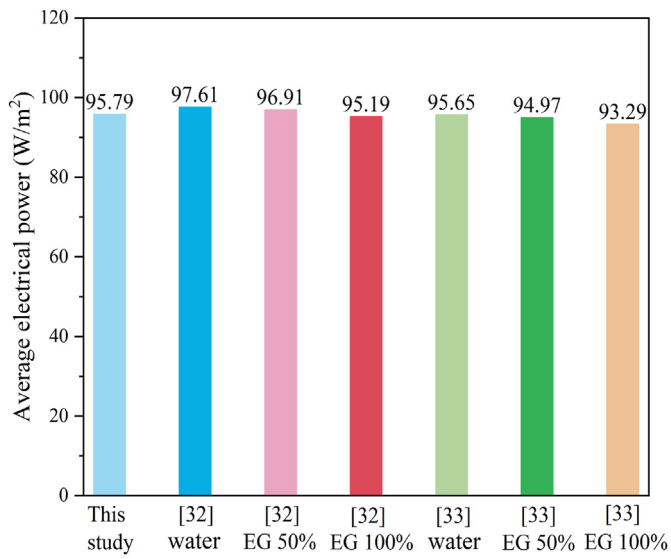

Fig. 13. Comparison with other works in average electrical power.

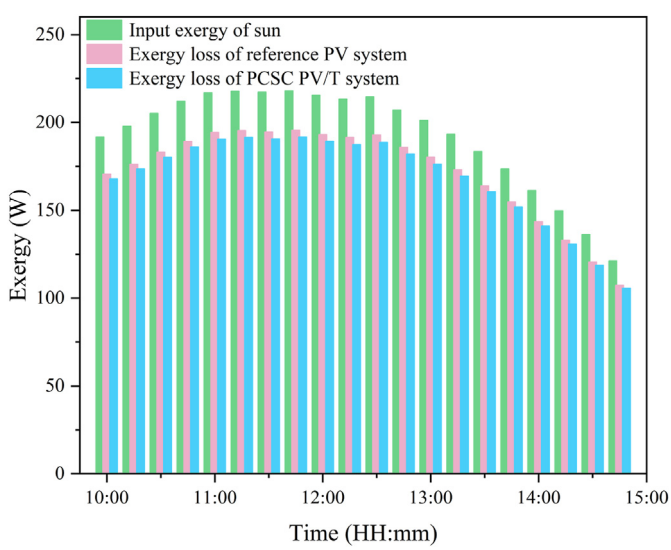

Fig. 14. The variation of input exergy and exergy loss of the PCSC PV/T module and the reference PV module.

also clear to figure out that the slope of the fitting line of the reference PV module is larger than that of the PCSC PV/T module under the solar radiation range of 500–1000 W/m^2.

3.5. Performance comparison of glazed and unglazed system

To compare the influence of adding glass cover on the systems. The performance of the unglazed and unglazed PCSC PV/T system is compared. For easy access to the examined systems, the mass flow rate of cooling water is fixed at 0.004 kg/s. In this section, four different cases are considered to make a comparison, namely reference PV module 1 (case 1), glazed PCSC PV/T module (case2), reference PV module 2 (case 3), unglazed PCSC PV/T module (case 4).

Fig. 17 reveals the average temperatures of the four cases, which are 57.98 °C, 40.12 °C, 61.275 °C, and 37.36 °C, respectively. It is apparent that the temperatures of the two PCSC PV/T modules are lower than those of the corresponding reference PV modules.

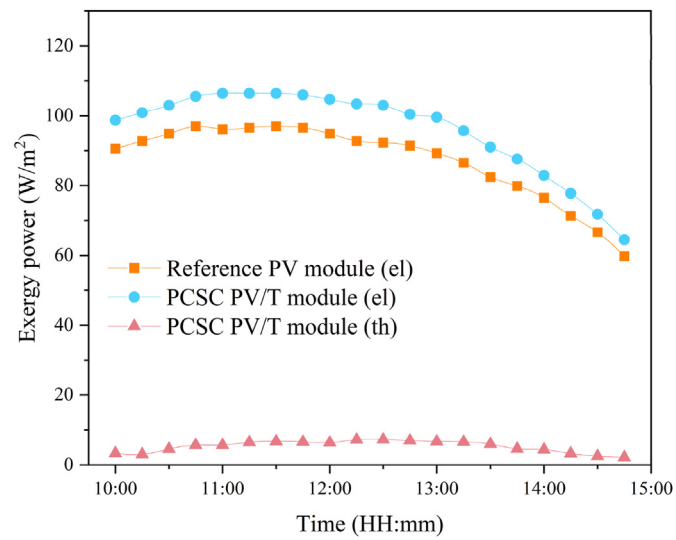

Fig. 15. The variation of input exergy and exergy loss of the PCSC PV/T module and the reference PV module.

Besides, the temperature of case 4 is lower than the temperature of case2.

Further information can be obtained by reviewing the IR imagines of the four cases, as shown in Fig. 18. For both systems, the reference PV modules possess higher temperature. Due to the existence of the glass cover, the thermal radiation emitted by the glazed PCSC PV/T module is quite lower than the unglazed PV/T module, which presents less heat loss.

The variations of the electrical power of the glazed and unglazed PCSC PV/T systems are demonstrated in Fig. 19 (a). The electricity yielded by the unglazed PCSC PV/T module is quite higher than that of the glazed PCSC PV/T module. The average electric powers are 85.7 W/m^2 and 91.0 W/m^2 for the glazed and unglazed systems. This result can be explained as: firstly, the covered glass plate leads to higher average PV module temperature, which worsens the working condition of the solar cells. Secondly, the glass cover results in optical loss during the transmission of solar irradiation. As depicted in Fig. 19 (b), an opposite result is presented, the thermal power of the glazed PCSC PV/T module is significantly higher than the unglazed PCSC PV/T module, with an average value of 275.2 W/m^2 and 239.4 W/m^2, respectively.

The variation of the short-circuit current is shown in Fig. 20. There is no doubt that the short-circuit current of the unglazed PCSC PV/T module exceeds the value of the glazed PCSC PV/T module. It is universal that the short-circuit current of silicon-based solar cells is more sensitive to solar radiation than the open circuit voltage. In addition, compared with the unglazed PCSC PV/T module, the short-circuit current loss is also presented in Fig. 20. The average short-circuit current loss of the glazed PCSC PV/T module is about 9%. The existence of a borosilicate glass cover will lead to an optical loss, which also confirms in previous results [35].

The composition of the overall input exergy and exergy losses of the two systems is presented in Fig. 21. From this figure, it can be obtained that the percentages of the overall output exergy (the sum of electrical exergy and thermal exergy) and the exergy losses of the unglazed and glazed PCSC PV/T module are 10.38%, 10.04%, 89.62%, and 89.96%, respectively. The relative percentage share of the exergy losses increases by 0.38% when using the glass cover. It is also evident that the thermal exergy of the system can be enhanced by using the glass cover, while the electrical exergy decreases.

Fig. 22 compares the entropy generation of the unglazed and

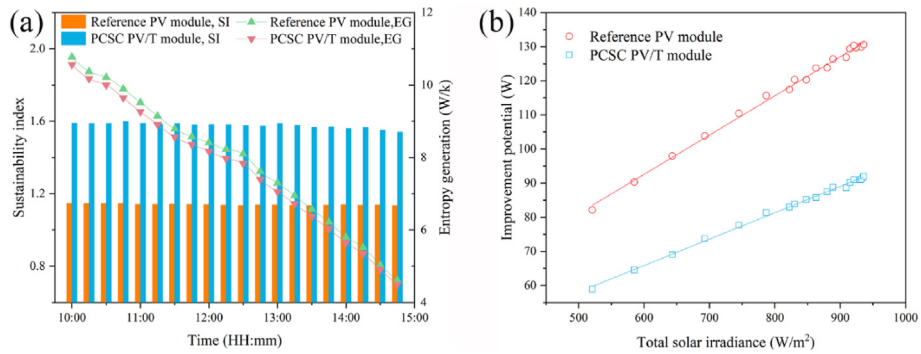

Fig. 16. The variation of (a) SI, entropy generation and (b) IP with total solar irradiance.

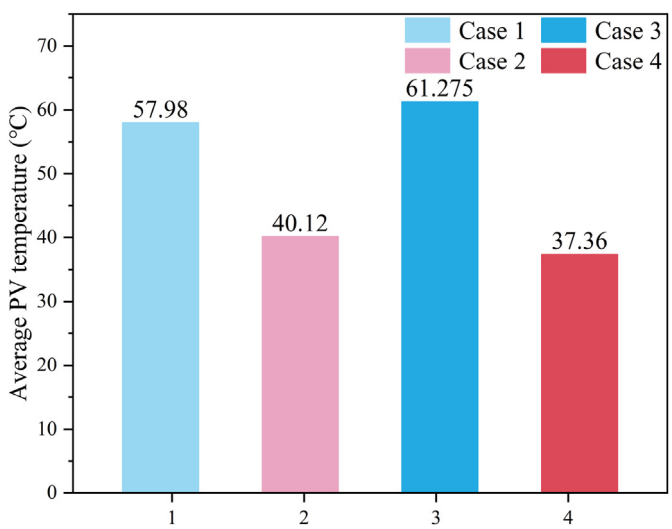

Fig. 17. The average temperature of the four considered cases.

glazed PV/T systems versus local time. It can be noted that the entropy generation of the unglazed PCSC PV/T module decreases from the start period of 10.62 W/k to the end of the value of 4.5 W/k, while the glazed PCSC PV/T module reduces from the initial value of 9.3 W/k to the end of 3.79 W/k. Besides, over the entire time range, the irreversibility of the glazed PCSC PV/T module is lower than the unglazed PCSC PV/T module, which can be interpreted by the fluid friction and heat transfer loss of the systems [32].

The performance comparison of the unglazed and glazed PCSC PV/T system are summarized in Table 5. It is clear to find out that the electrical performance of the unglazed PCSC PV/T system is superior to the glazed PCSC PV/T system, with an average daily electrical energy and efficiency of 91 W/m^2 and 10.76%, respectively. In contrast, the glazed PCSC PV/T system is better than the unglazed PCSC PV/T system in daily overall and thermal energy.

The reasons can be further explained as: From one hand, as previously discussed, the additional glass cover causes undesirable optical loss in the system, which is harmful to the production of electricity. On the other hand, the air gap between the upper surface of the PV module and the lower surface of the glass cover leads to a miniature "greenhouse effect" [32]. This reduces the heat loss of the system and increases the PV panel temperature, which further decreases the electrical efficiency of the system due to the sensitivity of the solar cell to temperature.

3.6. Economic analysis

For assessment of the economic performance of the proposed PCSC PV/T system, the levelized cost of electricity (LCOE) method recommended by International Renewable Energy Agency (IRENA) is considered in this study [36]. The expression of the LCOE model is described as follows:

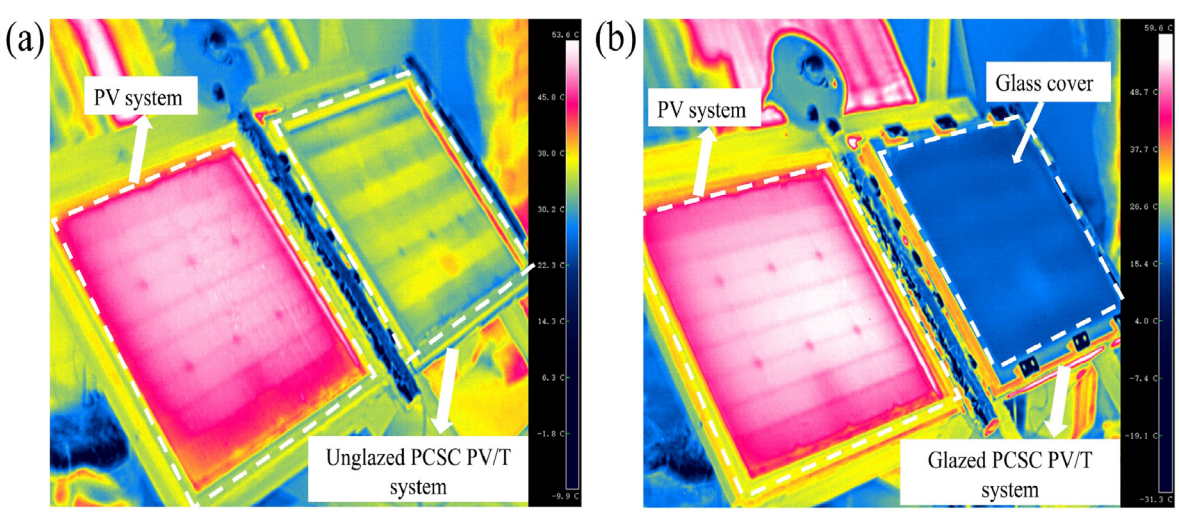

Fig. 18. The IR imagines of (a) the unglazed PV/T modules and (b) the glazed PV/T modules.

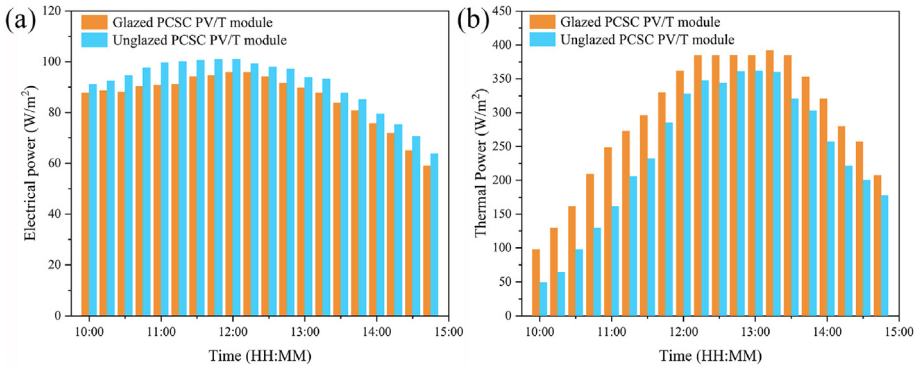

Fig. 19. The variations of (a) electrical power and (b) thermal power of the glazed/unglazed PCSC PVT systems.

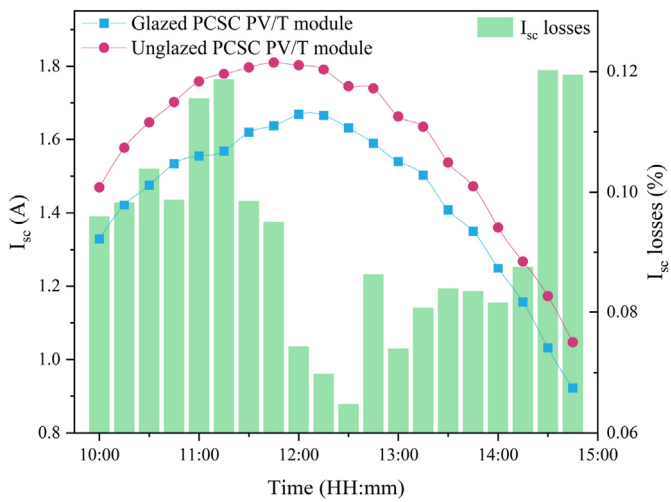

Fig. 20. The variations of the short-circuit current of the glazed and unglazed PCSC PV/T modules.

$$LCOE = \frac{\sum_{t=1}^{n} \frac{I_t + M_t + F_t}{(1+r)^t}}{\sum_{t=1}^{n} \frac{E_t}{(1+r)^t}} \tag{33}$$

$$E_t = E_0 \left(1 - \frac{DR}{100}\right)^t \tag{34}$$

where, I_t is investment cost in year, M_t is operations and maintenance expenditures in year, F_t is fuel expenditures in the year. r and n are discount rate and life time of the system. E_t and E_0 refer to the electricity generation in the year and the electricity produced in the first year of the installation. DR stand for degradation factor of the system. Generally, for renewable energy generation system, the fuel cost of F_t is usually considered as zero [37]. In addition, for PV/T systems, both thermal and electricity energy are produced. Therefore, a conversion factor of 0.55 is used to convert thermal energy to equivalent electricity, which represents the typical efficiency of a modern natural gas power plant [38].

Moreover, another economic metrics of net present value (NPV) is also considered in this study. The calculation formula of NPV is expressed as [39]:

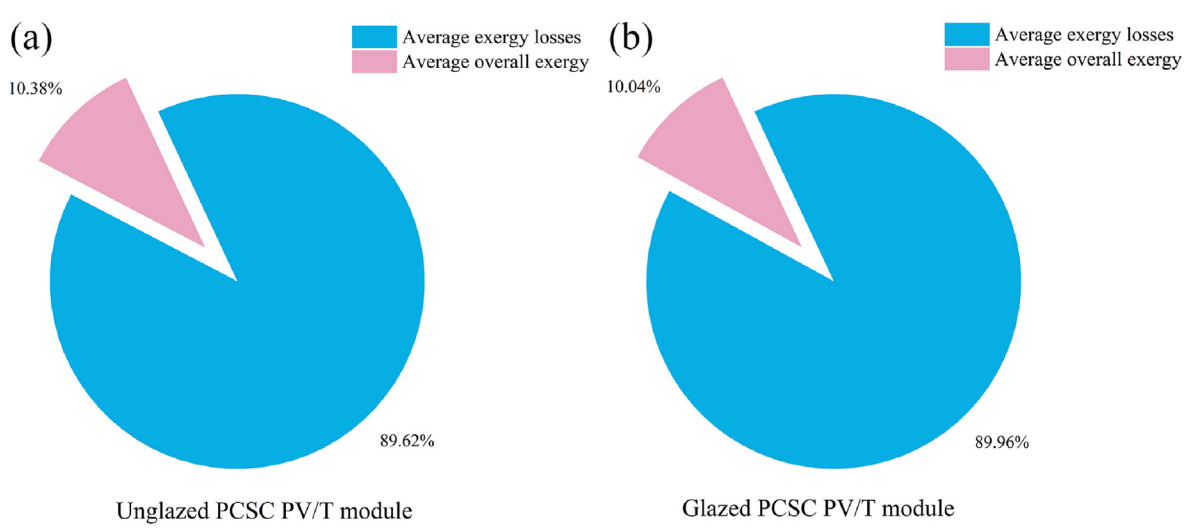

Fig. 21. The average overall exergy and exergy losses of (a) unglazed PCSC PV/T module (b) glazed PCSC PV/T module.

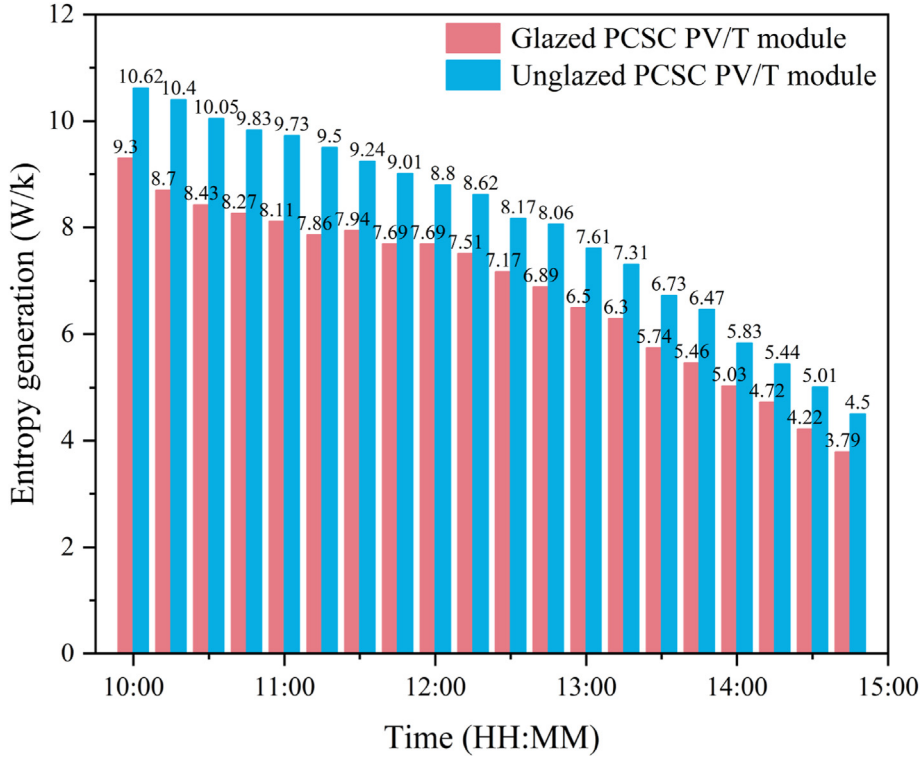

Fig. 22. The variations of entropy generation of the unglazed PCSC PV/T module and glazed PCSC PV/T module.

Table 5
Summarize of the performance of the glazed/unglazed PCSC PV/T system.

Evaluation parameters	Unglazed PCSC PV/T system	Glazed PCSC PV/T system
Average electrical power (W/m$^{2)}$	91.0	85.7
Average thermal power (W/m$^{2)}$	239.4	275.2
Total energy (W/m$^{2)}$	330.4	360.9
Average daily electrical efficiency (%)	10.76	10.16
Average daily thermal efficiency (%)	28.56	34.47

$$NPV = -TIC + \sum_{t=1}^{n} \frac{E_0 * Pr_{ele}}{(1+r)^t} \tag{35}$$

where, Pr_{ele} is the represent the electricity sale price in China. According to the guide tariff released by National Development and Reform Commission (NDRC) for PV generation system in 2016, the specific value of Pr_{ele} is taken as 0.1329 ($/kW h) [40]. The required economic parameters and obtained results are summarized in Table 6. By assuming an operation time of 25 years, the LCOE price for reference PV system is found to be 0.1485 ($/kW h) whereas by adopting PCSC technology, the LCOE price are reduced to 0.1211 ($/kW h) and 0.1327 ($/kW h) for unglazed and glazed PV/T systems. While, the NPV value for reference PV system, unglazed PCSC PV/T system, and glazed PV/T system are 37,404 $, 107,653 $, and 103,107 $ respectively. Therefore, from the above analysis, it can be found that the LCOE price of the proposed PV/T system is higher than the guide tariff of 0.1329 ($/kW h), and thus it could be concluded that the presented system is economically appropriate.

Table 6
Economic parameters evaluation of the PCSC PV/T system.

Economic parameters	Reference PV	Unglazed PCSC PV/T	Glazed PCSC PV/T
Production of equivalent electricity (kW h)	26.03	74.91	71.75
Total investment cost (*TIC*) ($)	18.76	44.04	46.22
Life time of system (n)	25	25	25
Degradation factor (DR) (%)	0.5	0.5	0.5
Discount rate (%)	7	7	7
Operation and maintenance cost (M_t) ($)	0.02*total investment cost	0.02*total investment cost	0.02*total investment cost
Installation cost (C_{ins}) ($)	0.1*total investment cost	0.1*total investment cost	0.1*total investment cost
Electricity sale price ($/kW h)	0.1329	0.1329	0.1329
Levelized cost of electricity (LCOE) ($/kW h)	0.1485	0.1211	0.1327
Net present value (NPV) ($)	37,404	107,653	103,107

4. Conclusion

In this study, a novel type of PCSC PV/T system based on PCC technology and porous media is proposed and experimentally investigated. The performance of the PCSC PV/T system is accessed by comparing it with the reference PV system from the energy, exergy, and economical viewpoints. It is worth noting that the experimental data are obtained under the conditions described in this study and may vary from other prescribed conditions. The main findings derived from this study are presented as follows:

1. The PCSC PV/T system has lower temperature in comparison with reference PV system. The maximum surface temperature difference of PCSC PV/T module is only 4.2 °C, whereas the reference PV module is 5.7 °C.
2. Compared with the reference PV system, the average percentage increase of electrical efficiency for PCSC PV/T system under different mass flow rates of 0.004 kg/s, 0.007 kg/s, 0.009 kg/s are 9.74%, 16.87%,15.06%, respectively. Meanwhile, the average increased electrical power is 2 W.
3. The overall energy efficiency of the PCSC-PV/T system improves with increasing mass flow rates. The maximum thermal and electrical energies for the PCSC PV/T system are 239.4 W/m^2 and 95.36 W/m^2, respectively.
4. For PCSC PV/T system, adding glass cover is beneficial to harvest thermal energy whereas adverse for producing electrical energy.
5. The economic analysis indicates that the LCOE price for reference system is 0.1485 ($/kW h), while the LCOE price for unglazed and glazed PCSC PV/T systems are reduced to 0.1211 ($/kW h) and 0.1327 ($/kW h) respectively, which makes it economically available.

Credit author contribution statement

Yuanzhi Gao: Conceptualization, Methodology, Formal analysis, Writing – original draft. **Guohao Hu:** Methodology, Formal analysis, Writing – original draft. **Yuzhuo Zhang:** Formal analysis, Writing – original draft. **Xiaosong Zhang:** Conceptualization, Supervision, Funding acquisition, Writing – review & editing.

Declaration of competing interest

The authors declare that they have no known competing financial interests or personal relationships that could have appeared to influence the work reported in this paper.

Acknowledgments

The research described in this paper is supported by the Key R & D Program of Jiangsu province (No.BE2018118), the National Natural Science Foundation of China (No.51876034). Acknowledgments are also given to Xutong Shen and Chao Yang, for their contribution to language editing and meaningful discussion in this paper.

References

[1] Rahman MM, Hasanuzzaman M, Abd Rahim N. Effects of operational conditions on the energy efficiency of photovoltaic modules operating in Malaysia [J]. J Clean Prod 2017;143:912–24.
[2] Al-Waeli A, Chaichan MT, Kazem HA, et al. Comparison study of indoor/outdoor experiments of a photovoltaic thermal PV/T system containing SiC nanofluid as a coolant[J]. Energy 2018;151:33–44.
[3] He Y, Hu Y, Li H. An Ag@ TiO2/ethylene glycol/water solution as a nanofluid-based beam splitter for photovoltaic/thermal applications in cold regions[J]. Energy Convers Manag 2019;198:111838.
[4] Savvakis N, Tsoutsos T. Theoretical design and experimental evaluation of a PV+PCM system in the Mediterranean climate[J]. Energy 2020.
[5] Barone G, Buonomano A, Forzano C, et al. Experimentation, modelling and applications of a novel low-cost air-based photovoltaic thermal collector prototype[J]. Energy Convers Manag 2019;195:1079–97.
[6] Maatallah T, Zachariah R, Al-Amri FG. Exergo-economic analysis of a serpentine flow type water based photovoltaic thermal system with phase change material (PVT-PCM/water) [J]. Sol Energy 2019;193:195–204.
[7] Hissouf M, Najim M, Charef A. Numerical study of a covered Photovoltaic-Thermal Collector (PVT) enhancement using nanofluids[J]. Sol Energy 2020;199:115–27.
[8] Grubišić-Čabo F, Nižetić S, Čoko D, et al. Experimental investigation of the passive cooled free-standing photovoltaic panel with fixed aluminum fins on the backside surface[J]. J Clean Prod 2018;176:119–29.
[9] Wang M, Peng J, Luo Y, et al. Comparison of different simplistic prediction models for forecasting PV power output: assessment with experimental measurements[J]. Energy 2021;224(11):120162.
[10] Bahaidarah HMS, Baloch AAB, Gandhidasan P. Uniform cooling of photovoltaic panels: a review[J]. Renew Sustain Energy Rev 2016;57:1520–44.
[11] Srm A, Hs A, Ak B, et al. Improving the performance of PV/T systems by using conical-leaf inserts in the coolant tubes[J]. Sol Energy 2020;212:84–100.
[12] Yuan X, Zhou X, Pan Y, et al. Phase change cooling in data centers: a review[J]. Energy Build 2021:110764.
[13] Suresh V, Naviynkumar S, Kirubakaran V. Improved power output of PV system by low cost evaporative cooling technology[C] 2013 International Conference on Green Computing, Communication and Conservation of Energy (ICGCE). IEEE 2013:640–3.
[14] Alami AH. Effects of evaporative cooling on efficiency of photovoltaic modules [J]. Energy Convers Manag 2014;77:668–79.
[15] Nižetić S, Čoko D, Yadav A, et al. Water spray cooling technique applied on a photovoltaic panel: the performance response[J]. Energy Convers Manag 2016;108:287–96.
[16] Maatallah T, Zachariah R, Al-Amri FG. Exergo-economic analysis of a serpentine flow type water based photovoltaic thermal system with phase change material (PVT-PCM/water) [J]. Sol Energy 2019;193:195–204.
[17] Fayaz H, Rahim NA, Hasanuzzaman M, et al. Numerical and experimental investigation of the effect of operating conditions on performance of PVT and PVT-PCM[J]. Renew Energy 2019;143:827–41.
[18] Ahmed OK, Mohammed ZA. Influence of porous media on the performance of hybrid PV/Thermal collector[J]. Renew Energy 2017;112:378–87.
[19] Wang Y, Gao Y, Huang Q, et al. Experimental study of active phase change cooling technique based on porous media for photovoltaic thermal management and efficiency enhancement[J]. Energy Convers Manag 2019;199:111990.
[20] Feng C, Chandra S. Evaporation of ethanol films wicking on structured, porous coatings deposited on copper plates[J]. Int J Heat Mass Tran 2019;136:821–31.
[21] Preet S, Bhushan B, Mahajan T. Experimental investigation of water based photovoltaic/thermal (PV/T) system with and without phase change material (PCM)[J]. Sol Energy 2017;155:1104–20.
[22] Kazemian A, Hosseinzadeh M, Sardarabadi M, et al. Experimental study of using both ethylene glycol and phase change material as coolant in photovoltaic thermal systems (PVT) from energy, exergy and entropy generation viewpoints[J]. Energy 2018;162:210–23.
[23] Sardarabadi M, Passandideh-Fard M, Heris SZ. Experimental investigation of the effects of silica/water nanofluid on PV/T (photovoltaic thermal units) [J]. Energy 2014;66:264–72.
[24] Ozden E, Tari I. Energy–exergy and economic analyses of a hybrid solar–hydrogen renewable energy system in Ankara, Turkey[J]. Appl Therm Eng 2016;99:169–78.
[25] Sardarabadi M, Hosseinzadeh M, Kazemian A, et al. Experimental investigation of the effects of using metal-oxides/water nanofluids on a photovoltaic thermal system (PVT) from energy and exergy viewpoints[J]. Energy 2017;138:682–95.
[26] Chow TT, Pei G, Fong KF, et al. Energy and exergy analysis of photovoltaic–thermal collector with and without glass cover[J]. Appl Energy 2009;86(3):310–6.
[27] Caliskan H. Energy, exergy, environmental, enviroeconomic, exergoenvironmental (EXEN) and exergoenviroeconomic (EXENEC) analyses of solar collectors[J]. Renew Sustain Energy Rev 2017;69:488–92.
[28] Xu H, Wang N, Zhang C, et al. Energy conversion performance of a PV/T-PCM system under different thermal regulation strategies[J]. Energy Convers Manag 2021;229:113660.
[29] Chandrasekar M, Suresh S, Senthilkumar T. Passive cooling of standalone flat PV module with cotton wick structures[J]. Energy Convers Manag 2013;71:43–50.
[30] Bahaidarah H, Subhan A, Gandhidasan P, et al. Performance evaluation of a PV (photovoltaic) module by back surface water cooling for hot climatic conditions[J]. Energy 2013;59:445–53.
[31] Rahman MM, Hasanuzzaman M, Rahim NA. Effects of various parameters on PV-module power and efficiency[J]. Energy Convers Manag 2015;103:348–58.
[32] Kazemian A, Taheri A, Sardarabadi A, et al. Energy, exergy and environmental

analysis of glazed and unglazed PVT system integrated with phase change material: an experimental approach[J]. Sol Energy 2020;201:178–89.
[33] Kazemian A, Hosseinzadeh M, Sardarabadi M, et al. Experimental study of using both ethylene glycol and phase change material as coolant in photovoltaic thermal systems (PVT) from energy, exergy and entropy generation viewpoints[J]. Energy 2018;162:210–23.
[34] Kazemian A, Hosseinzadeh M, Sardarabadi M, et al. Effect of glass cover and working fluid on the performance of photovoltaic thermal (PVT) system: an experimental study[J]. Sol Energy 2018;173:1002–10.
[35] Zhang W, Chen M, Zhang S, et al. Designation of a solar falling-film photochemical hybrid system for the decolorization of azo dyes[J]. Energy 2020;197:117182.
[36] International Renewable Energy Agency (IRENA). Renewable Energy Technologies: Cost analysis series. Volume 1, Power Sector, Issue 4/5, Solar Photovoltaics <https://www.irena.org/publications/2012/Jun/Renewable-Energy-Cost-Analysis-Solar-Photovoltaics. Accessed 24 June 2021>, 2012.
[37] Abdelhady S. Performance and cost evaluation of solar dish power plant: sensitivity analysis of levelized cost of electricity (LCOE) and net present value (NPV) [J]. Renew Energy 2021;168:332–42.
[38] Wang K, Herrando M, Pantaleo AM, et al. Technoeconomic assessments of hybrid photovoltaic-thermal vs. conventional solar-energy systems: case studies in heat and power provision to sports centres[J]. Appl Energy 2019;254:113657.
[39] Zayed ME, Zhao J, Li W, et al. Performance prediction and techno-economic analysis of solar dish/stirling system for electricity generation[J]. Appl Therm Eng 2020;164:114427.
[40] Central People's Government of the People's Republic of China. National Development and Reform Commission on the adjustment of photovoltaic power generation onshore wind power benchmark feed-in tariff notice. <http://www.gov.cn/xinwen/2016-12/28/content_5153820.htm. Accessed 24 June 2021>. 2016.